



Eco-friendly Fabrication of Polymer Encapsulated Gold Nanoparticles with Anticancer and Antimicrobial activities

MANSI CHAUDHARY^{1*}, LEELA CHAUDHARY¹, NIDHI PATEL¹,
HIMANI MOGA¹, KOKILA A. PARMAR² and CHIRAG MAKVANA¹

¹Department of Chemistry, Gokul Global University, Siddhpur, Gujarat 384151, India.

²Department of Chemistry, Hemchandracharya North Gujarat University,
Patan, Gujarat 384265, India.

*Corresponding author E-mail: chaudharimansi284@gmail.com

<http://dx.doi.org/10.13005/ojc/400611>

(Received: October 16, 2024; Accepted: December 14, 2024)

ABSTRACT

Polyvinylpyrrolidone (PVP) encapsulated gold nanoparticles (AuNPs) have gained significant attention in biomedical research due to their unique physicochemical and therapeutic properties. This study outlines an eco-friendly approach for synthesizing PVP-AuNPs using *Gymnema sylvestre* extract as a natural reducing agent. By optimizing the extract to HAuCl₄ ratio, effective synthesis was achieved at a 3.0% extract concentration producing spherical AuNPs with an average size of 33 nm as confirmed by transmission electron microscopy (TEM). Fourier transform infrared spectroscopy (FTIR) analysis validated the successful encapsulation of AuNPs with PVP revealing characteristic peaks corresponding to PVP and functional groups from the plant extract. Furthermore, X-ray diffraction (XRD) patterns confirmed the crystalline nature of the synthesized AuNPs. The PVP-AuNPs exhibited cytotoxic activity against HeLa cancer cells, with an IC₅₀ value of 32.42 µg/mL after 48 hours. Additionally, the nanoparticles demonstrated significant bactericidal activity against pathogens such as *Pseudomonas aeruginosa*, *Escherichia coli*, *Bacillus subtilis*, and *Staphylococcus aureus*, showing concentration-dependent antimicrobial effects. This work underscores the potential of green-synthesized PVP-AuNPs as a versatile platform for cancer therapy and antimicrobial applications providing a sustainable pathway to advancements in nanomedicine.

Keywords: Gold nanoparticles, Green synthesis, Anticancer, Antimicrobial.

INTRODUCTION

Among other nanomaterials, gold nanoparticles (AuNPs) have unique and advantageous properties that make them extremely important in the field of biomedicine. AuNPs are highly versatile and find broad applications due to their capacity to readily conjugate with various

molecules including drugs, oligonucleotides and antibodies. AuNPs possess a distinct surface plasmon resonance (SPR) that offers remarkable photo stability and effective light absorption. Because of this property, AuNPs are perfect for a variety of biological and medicinal uses, including gene and drug delivery, tissue engineering and cancer nanotechnology¹.



Green synthesis is a relatively recent field of research that focus on creating environmentally friendly techniques for producing nanostructures that are of high quality and can be sustained commercially. Biological systems including plant extracts, fungi and microbes are considered highly effective and economical approaches for synthesizing AuNPs primarily because of their straightforward and sustainable nature. This technology is ecologically sustainable since it completely eliminates the utilization of hazardous chemicals throughout the synthesis process. Several plant species and their extracts have been recognized as possible agents that can reduce and cap AuNPs during manufacture. The synthesis of AuNPs employing plant extracts such as *Sorbusaucuparia*, sugar beet pulp, *Hibiscus rosa-sinensis*, *Mangifera indica*, *Syzygium aromaticum*, *Anacardium occidentale* and *Murrayakoenigii* has been well documented in literature²⁻⁸.

The ability of bacteria, chemicals, insects and their byproducts and plant extracts to synthesis AuNPs has been thoroughly studied. Various synthesis techniques utilizing plant extracts can yield AuNPs with distinct characteristics. The efficacy of each plant extraction process is mostly determined by the unique composition and characteristics of the plant species employed which subsequently impact the size and properties of the produced AuNPs. These methods are well-known for being environmentally friendly, economically efficient and compatible with living organisms^{9,10}.

Chandran *et al.*, created gold nano triangles using aloe vera extract, attributing their formation to the extract's carbonyl compounds and the gradual reduction of gold ions.¹¹ In a similar manner, Talib *et al.*, utilized aloe vera extract to diminish and stabilize AuNPs examining their physicochemical characteristics in different physiological circumstances. They discovered that stable complexes were predominantly generated within the pH range of neutral to slightly acidic¹². Philip *et al.*, conducted a groundbreaking work where they utilized honey to carry out the green synthesis of AuNPs. The study indicated that fructose played a role in facilitating the reduction process while proteins were responsible for stabilizing the AuNPs¹³. In their study, Nakkala *et al.*, utilized *Gymnema sylvestre* extract to manufacture Ag and AuNPs. They

discovered that these NPs had significant cytotoxicity and antioxidant action against the Hep2 cell line.¹⁴

Significant research has explored the use of AuNPs in chemotherapy, cancer cell diagnostics, and as probes for microscopic analysis of cancer cells. Researcher have underlined that the cytotoxic and anti-proliferative effects of these substances can differ depending on factors such as the kind of cells, the size of the particles, and the concentration. Priya and Iyer observed that the effectiveness of biosynthesized NPs against MCF-7 breast cancer cell lines varied depending on the dosage. Nevertheless, the utilization of *Sphagneticola trilobata* leaves for the synthesis of AuNPs has not been previously investigated. Their work was to produce AuNPs using the process of green synthesis, utilizing a water-based extract derived from the leaves. Additionally, the study attempted to evaluate the effectiveness of these AuNPs in combating colon cancer cell lines (HCT-15) with potential anticancer capabilities¹⁵.

Recently, there has been a significant increase in the integration of ethno-botanical knowledge into the study of medicinal plants particularly within certain scientific communities. *Gymnema sylvestre* was chosen as a key plant traditionally used by the Kanitribals in the Tirunelveli hills of the Western Ghats, Tamil Nadu in India due to its historical significance and therapeutic properties¹⁶. *Gymnema sylvestre* also known as "Meshasringi" is extensively found in India and is highly esteemed in traditional medicine for its stomachic, diuretic and anti-diabetic properties. This adolescent shrub is distinguished by its young stems and branches. It has leaves that grow in pairs in a certain pattern with each leaf being either oval or elliptical in shape and measuring between 2.5 and 6 cm in length. The plant exhibits the production of little yellow flowers arranged in clusters known as umbellate cymes. Additionally, its elongated follicles, which have a lanceolate shape can reach a length of up to 3 inches^{17,18}.

Gymnema sylvestre is renowned for its adaptability in traditional medicine particularly in India where it has been extensively utilized for the treatment of diabetes¹⁹. *Gymnema sylvestre* possesses diverse bioactive components that effectively treat various conditions including asthma, eye disorders, snakebites, cough, respiratory

issues, pain, heart ailments, hemorrhoids and hepatosplenomegaly in addition to its anti-diabetic properties. Additionally, it is employed in the context of family planning. Antibacterial, anticancer, anti-obesity, anti-inflammatory, anti-hyperglycemic, antiulcer, anti-stress and anti-allergic qualities are also demonstrated by it. Utilizing bioactive components derived from medicinal plants which frequently imitate chemical substances continues to be a crucial strategy in the treatment of diverse disorders²⁰.

Gymnema sylvestre extract was used as a natural reducing agent in this study to create AuNPs which were then encapsulated with PVP to increase their stability and biocompatibility. The produced PVP-AuNPs were fully characterized using a range of analytical techniques to assess their optical, morphological and structural properties. The biological potential of these PVP-AuNPs was further explored focusing on their evaluation of the cytotoxic effects of the PVP-AuNPs on HeLa cells and antimicrobial activity which opens new avenues for biomedical applications.

MATERIALS AND METHODS

Materials and reagents

The dried leaves and stems of *Gymnema sylvestre* were sourced from local herbal markets. Gold (III) chloride trihydrate ($\text{HAuCl}_4 \cdot 3\text{H}_2\text{O}$, 99.9% purity) was obtained from Sigma-Aldrich. All other reagents used in this study, including ammonium hydroxide, Dulbecco's Modified Eagle Medium (DMEM), phosphate-buffered saline (PBS), 3-(4,5-dimethylthiazol-2-yl)-2,5-diphenyl tetrazolium bromide (MTT), fetal bovine serum (FBS), dimethyl sulfoxide (DMSO), nutrient broth, Mueller-Hinton agar, and bacterial strains (*Pseudomonas aeruginosa*, *Escherichia coli*, *Bacillus subtilis*, and *Staphylococcus aureus*) were procured from Sigma-Aldrich and ACROS Organics. Additionally, polyvinylpyrrolidone (PVP) and Alamar Blue (Resazurin) were also sourced from the same suppliers for immediate use.

Preparation of aqueous extract

The *Gymnema sylvestre* leaves were thoroughly washed, shade-dried for two weeks and ground into a fine powder. A 20 g portion of the powder was combined with 100 mL of distilled water and heated at 60°C for 30 minutes. The resulting

mixture was then agitated in the dark at 30°C. After filtration the extract was collected and stored in a sealed container for future use.

Green synthesis of PVP-AuNPs

Gymnema sylvestre extract was added in different amounts to a flask containing 1.0 mM $\text{HAuCl}_4 \cdot 3\text{H}_2\text{O}$ at pH 2.75. For one minute, the mixture was circulated at 250 rpm while being maintained at 30°C. With a total volume of 20 mL the extract concentrations ranged from 1.0% to 6.0% (%v/v). The final samples were classified as AuNPs 1.0%, AuNPs 2.0%, AuNPs 3.0%, AuNPs 5.0% and AuNPs 6.0% based on the extract ratio. The solution containing AuNPs was centrifuged for 30 min at 10,000 rpm. It was then stored for later use in a volume of 20 mL of Milli-Q water at 4°C after undergoing multiple washes with the water.²¹

Synthesis of PVP Encapsulated PVP-AuNPs

A total of 0.5 g of PVP was dissolved in 250 mL of Milli-Q water and stirred for one hour at a temperature between 60 and 80°C. AuNPs solution (150 mL) was progressively mixed with aqueous PVP. An hour or so later, a color shift was noticed. Centrifugation of the PVP-AuNPs-containing solution was performed for 30 min at 10,000 revolutions per minute. Subsequently, it was subjected to several washes using Milli-Q water and then stored in a volume of 20 mL of Milli-Q water at a temperature of 4°C for future utilization²¹.

Characterization

The optical properties of the synthesized PVP-AuNPs samples were evaluated using a UV-Visible spectrophotometer (Shimadzu-1800) over the wavelength range of 450 to 650 nm. Their morphology, including size and shape was characterized through transmission electron microscopy (TEM) using a JEM1010-JEOL model. A small amount of the re-dispersed PVP-AuNPs suspension in water was placed on a carbon-coated copper grid and air dried prior to TEM analysis. The crystallinity of the samples was assessed by X-ray diffraction (XRD) with a Miniflex Rigaku 600 instrument, operating at 30 kV and 2 mA, with a scanning speed of 10° per minute. The XRD measurements were taken across a 2θ range of 3-90° utilizing Cu-Kα radiation and a graphite monochromator. Fourier transform infrared (FT-IR) spectroscopy (Shimadzu-8400) was employed to identify the main functional groups on the surfaces

of *Gymnema sylvestre* and PVP-AuNPs with spectra recorded in the range of 4000–500 cm^{-1} .

Anticancer activity by MTT assay

The MTT assay was used to measure the IC_{50} in HeLa cells in order to assess the anticancer activity of the PVP-AuNPs. The test formulation was sterilized with a 0.22 μm filter and sterility was confirmed by incubating 10 μL of extract in DMEM at 37°C for 24 hours. If no contamination was observed the extract was used for cell culture. On the day of treatment the test compounds were added to the wells and after incubation the media was replaced with 100 μL of PBS. Following two rounds of washing 20 μL of MTT solution and new medium were added and the mixture was then incubated for three hours at 37°C. The unbound MTT was then removed and the cells were washed with PBS before adding 100 μL of DMSO to dissolve any insoluble compounds. Absorbance was measured at 570 nm. The results (mean \pm SD, $n=3$) were analyzed using Excel, with groups assigned to control and treatment conditions.

Table 1: Experimental design of MTT assay

No	Group	Dose conc. (μg)	Dose (μL)	Media (μL)	Final dose conc. (μg)	No. of replicates
1	Control	0	1	199	0	3
2	Dose	10	1	199	10	3
3	Dose	25	1	199	25	3
4	Dose	50	1	199	50	3
5	Dose	75	1	199	75	3
6	Dose	100	1	199	100	3
7	PC	40.7	1	199	40.7	3

Antimicrobial activity

The antimicrobial activity of biosynthesized PVP-AuNPs was tested against *Gram-positive* and *Gram-negative* bacteria. In brief, 50 μL of broth medium was placed in each well of a 96-well plate, and the test materials were serially diluted in broth to concentrations ranging from 0.254 to 5000 $\mu\text{g}/\text{mL}$. A final inoculum of $0.5\text{--}2.5 \times 10^8$ CFU/mL was added. Controls included media only, bacterial growth control, and solvent control. The plates were incubated at 37°C for 20 h, followed by the addition of 30 μL of resazurin and 30-min incubation. By monitoring the color shift, the minimum inhibitory concentration (MIC) was ascertained.

RESULTS AND DISCUSSION

UV-Visible spectrometer

UV-Visible absorption spectroscopy, a highly effective method is frequently used to

observe the optical characteristics of particles that are quantum-sized²⁴. Fig. 1 demonstrates that the highest band associated with the distinct SPR occurs at around 545 nm. The existence of a maximal absorbance band at around 545 nm verifies the formation of PVP-AuNPs as it is a particular signal of their presence. Furthermore, the alteration in color of the solution from yellow to ruby-red following the reaction indicated the successful formation of PVP-AuNPs^{25,26}. Furthermore, the SPR band displayed a little displacement towards a longer wavelength when the extract ratios from *Gymnema sylvestre* increased, which is in line with the observed alteration in color. The data shows that the size of the AuNPs grew as the extract ratios climbed from 2.0% to 6.0%, with the exception of the 1.0% ratio (Fig. 1). The average diameters of the AuNPs rose in the following sequence: 2.0% < 3.0% < 5.0% < 6.0%. Singh and srivastava reported comparable phenomena. Significantly, the SPR band exhibited increased width when the extract ratio beyond 3.0% (specifically, at 5.0% and 6.0%) as a result of the formation of sizable anisotropic particles^{27,28}. Therefore, the sample PVP-AuNPs 3.0% was chosen for more investigations into its properties and its ability to inhibit cancer growth.

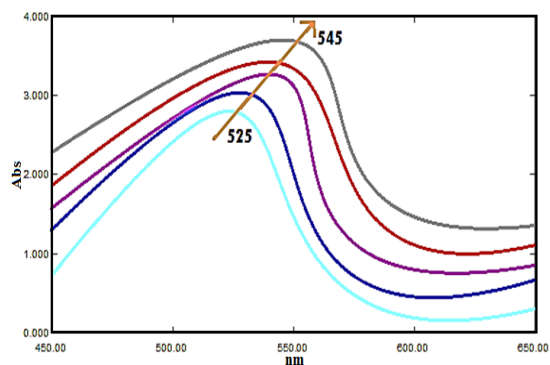


Fig. 1. UV-Visible spectra of the synthesized PVP-AuNPs

Fourier transforms infrared spectroscopy (FTIR)

The purpose of doing FTIR analysis was to examine the biomolecules present in *Gymnema sylvestre* extract that contribute to the synthesis of PVP-AuNPs was shown in Fig. 2. The band seen at 3429 cm^{-1} in PVP-AuNPs generated from *Gymnema sylvestre* matches to the stretching vibration of alcohols (O–H), indicating a strong connection. The band appears broad in nature. The major alcohol bands appear at 2935 cm^{-1} , while the band at 1720 cm^{-1} corresponds to the N=C=S stretching. The C=C band is associated with conjugated alkenes found in amide bonds within proteins. The *Gymnema sylvestre* produced

PVP-AuNPs exhibited clear characteristics of isothiocyanate and alkene groups. The C–Br stretching observed at 638 cm^{-1} was a result of the initial mixing with KBr during processing. The presence of these groups on PVP-AuNPs prevents them from clumping together by covering the unbound amino groups, which in turn makes the biosynthesized PVP-AuNPs more stable²⁹.

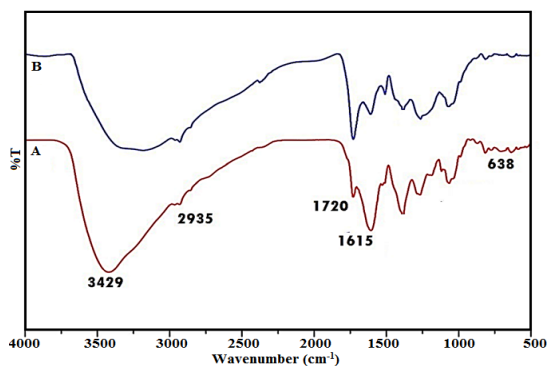


Fig. 2. FTIR spectra of (A) *Gymnema sylvestre* extract and (B) PVP-AuNPs

X-ray diffraction (XRD)

The higher crystallinity observed in the PVP-AuNPs 3.0% sample, as indicated by the distinct XRD peaks, can be attributed to the effective stabilization and controlled growth of AuNPs. PVP acts as stabilizing agent facilitating the formation of well-ordered crystalline structures during NPs synthesis. The specific XRD peaks at $2\theta^\circ$ values corresponding to the (111), (200), (220) and (311) planes suggest that the NPs have adopted a highly regular, face-centered cubic (FCC) lattice structure, which is typical for gold. This crystallinity is essential for the stability and functional properties of the NPs.³⁰ According to Malik *et al.*, standard diffraction bands demonstrated that the cubic phase of AuNPs displayed a face-centered orientation²⁹.

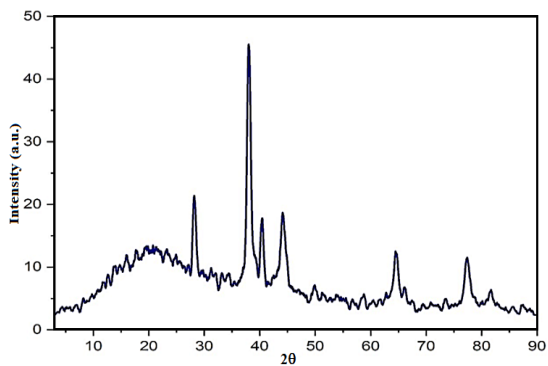


Fig. 3. XRD pattern of PVP-AuNPs

Transmission electron microscopy (TEM)

The synthesised PVP-AuNPs' size, shape,

and morphology were examined using the TEM technique. Fig. 4 demonstrates that PVP-AuNPs 3.0% displayed spherical shapes. Singh and Srivastava have reported similar observations when synthesizing PVP-AuNPs using black cardamom²⁸. The plant extract likely contributed to the successful stabilization of the particles, resulting in strongly mono-dispersed and non-agglomerated spheres or triangles²¹. These compounds have the ability to function as important ligands that enclose the PVP-AuNPs. Prior research has shown that the round structure of typical NPs can amplify their ability to kill germs, as observed with silver NPs and gold NPs^{31,32}. The PVA-AuNPs' particle sizes ranged from 17 to 45 nm, according to TEM examination. The majority of NPs were between the 30-35 nm range with a central value of 33 nm (Figure 4c).

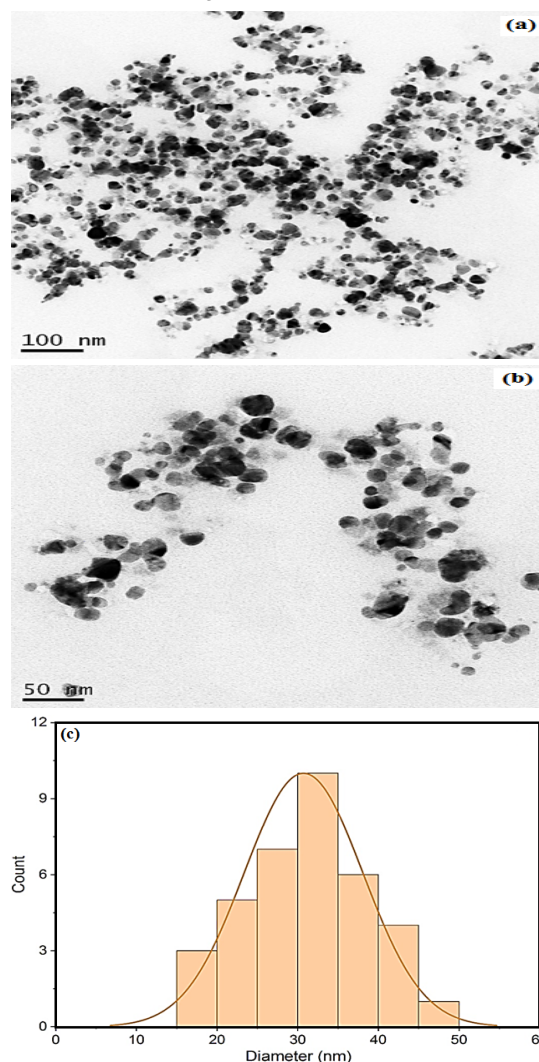


Fig. 4. (A and B) TEM images of PVP-AuNPs and (C) distribution of its particle diameter

Anticancer activity of PVP-AuNPs

PVP-AuNPs are substances used in cancer treatment that are becoming more and more well-liked in the medical community. There is a lack of study on the deadly impacts of biosynthesized PVP-AuNPs on cancer cell lines³³. The impact of PVP-AuNPs on the proliferation of HeLa cells was evaluated using the MTT assay. This study suggests that the inhibition of cell proliferation by biosynthesized PVP-AuNPs may be attributed to the induction of various forms of cell death. The test formulation's results were shown to differ based on its capacity to inhibit cellular dehydrogenase activity. The concentration of 10 μg demonstrated the most

minimal inhibition, with a measurement of around $33.18 \pm 1.56\%$. The highest degree of inhibition was seen at a dosage of 100 μg , with an approximate inhibition rate of $95.11 \pm 1.32\%$. The IC_{50} value was calculated using the equation $y = 0.6709x + 28.247$, yielding an approximate value of 32.42 μg . The harmful effects of test chemical were assessed on the HeLa cell line using the MTT assay. The study found that the mortality rate of cells, or the degree of inhibition of cell growth in the HeLa cell line, was contingent upon the dosage. To summarize, the experimental results showed the impressive ability of PVP-AuNPs to effectively combat cancer in the HeLa cell line.

Table 2: Data of MTT assay against HeLa cell line

Sr. No	Treatment (μg)	Group 1 (%)	Group 2 (%)	Group 3 (%)	Avg (%)	SD	SE
1	10	30.15	34.02	35.37	33.18	2.71	1.56
2	25	50.05	47.88	45.18	47.70	2.44	1.41
3	50	58.69	63.91	59.86	60.82	2.74	1.58
4	75	80.56	79.12	76.87	78.85	1.86	1.07
5	100	97.66	94.42	93.25	95.11	2.28	1.32

Sr. No	PC(5FU)(μg)	%of cell growth inhibition			Avg. (%)	SD	SE
		Group-1 (%)	Group-2 (%)	Group-3 (%)			
1	40.7	50.25	48.82	51.77	50.28	1.47	0.85

The outcomes show a dose-dependent increase in cell viability with the treatments, suggesting a clear pattern in which higher concentrations lead to increased cell viability. The positive control consistently demonstrated an inhibitory effect on cell growth, in accordance with anticipated results. These data indicate that the therapies used had a substantial effect on the survival of cells, and the variations shown at different concentrations are statistically significant due to the small standard errors.

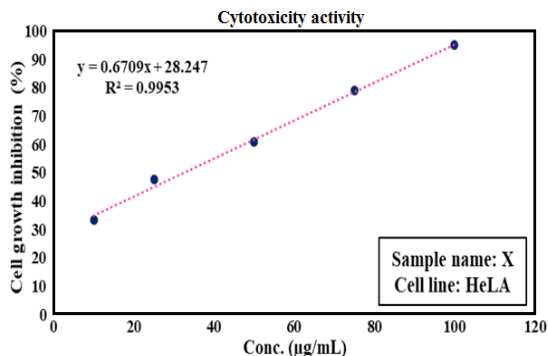


Fig. 5. % of cell growth inhibition at different concentration of test compound PVP-AuNPs (X)

Furthermore, the HeLa cells treated

with PVP-AuNPs exhibited cytotoxicity that was dependent on the dose. The findings demonstrated that cell viability decreased as PVP-AuNP concentrations increased, particularly in the 100 $\mu\text{g}/\text{mL}$ group, where almost all cells were impacted, leaving only about 10% viability. The biosynthesized PVP-AuNPs have an inhibitory concentration (IC_{50}) value of 32.42 $\mu\text{g}/\text{mL}$ after 48 h, resulting in a 50% mortality rate of HeLa cells (Fig. 5). Previous studies have shown that the amphiphilic nature of PVP-AuNPs promotes efficient cell membrane penetration and boosts metabolic activity. These factors lead to the production of reactive oxygen species (ROS), which subsequently trigger a hypoxic condition in cancer cells. The hypoxic condition exerts an inhibitory effect on metabolic functions and disrupts endothelial balance, ultimately suppressing cell growth and proliferation at different concentrations^{33,34}. Furthermore, it is believed that the components of *Celastrus hindsii* extract also play a role in preventing cancer^{35,36}, and when biomolecules are applied on the surface of PVP-AuNPs, they can be used to transport drugs³⁷.

Antimicrobial activity

Figure 6 illustrates the concentration-dependent response observed in all bacterial strains when the antimicrobial activity of PVP-AuNPs against *Escherichia coli*, *Pseudomonas aeruginosa*, *Staphylococcus aureus*, and *Bacillus subtilis* was assessed across a range of concentrations. At lower concentrations, the PVP-AuNPs were either ineffective or stimulated bacterial growth, as shown by negative inhibition percentages, possibly due to the insufficient NPs dose to disrupt critical cellular functions. However, at higher concentrations, PVP-AuNPs effectively inhibited bacterial growth, with a shift to positive inhibition percentages indicating the presence of a threshold concentration where PVP-AuNPs become bactericidal. The

antimicrobial activity of PVP-AuNPs could be attributed to several mechanisms, such as their ability to penetrate bacterial cell walls, generate ROS, or interfere with intracellular metabolic pathways. *Gram-negative* bacteria typically have a more complex cell wall structure compared to *Gram-positive* bacteria, which might explain why a higher concentration of PVP-AuNPs was necessary to observe a notable inhibition for strains like *Pseudomonas aeruginosa* and *Escherichia coli*. Moreover, the variance in inhibitory percentages at lower doses may be related to the NPs' size and surface chemistry, which influence their interactions with bacterial cells. Further investigations could focus on optimizing NPs size and surface modifications to enhance antimicrobial efficacy at lower concentrations.

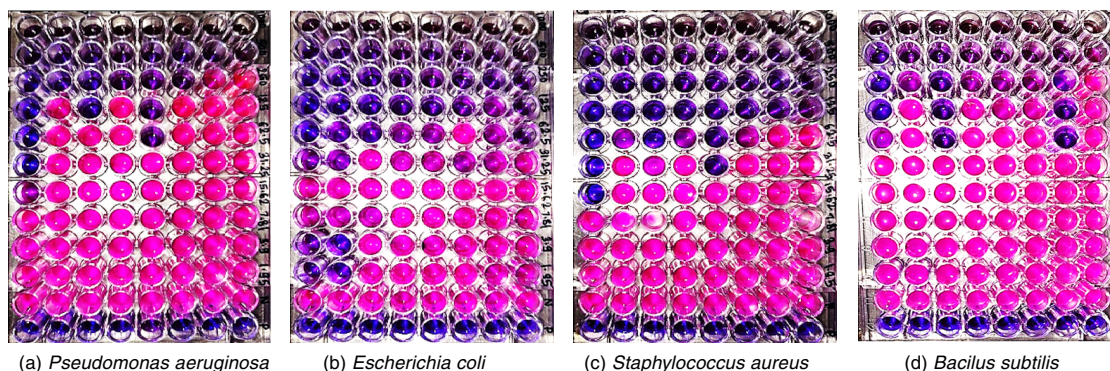


Fig. 6. Antimicrobial susceptibility test against *Gram-positive* and *Gram-negative* bacteria

CONCLUSION

A successful method for synthesizing stable, spherical-shaped PVP-AuNPs using *Gymnema sylvestri* extract has been formed. This process is straightforward, cost-effective, and non-toxic. The extraction ratio had a critical role in regulating the size distribution of the nanoparticles. The reduction of Au^3 took place swiftly at ambient temperature, and the resulting PVP-AuNPs remained stable over a period of time. By looking for recognizable bands in the XRD pattern, their crystalline structure was confirmed. The extract's phenolic and polyphenolic compounds were in charge of stabilizing and capping the PVP-AuNPs, according to the FTIR spectra. The abundant presence of phenolic compounds in *Gymnema sylvestri*, combined with its strong antioxidant properties, enabled the conversion of Au cations into AuNPs. Furthermore, the cytotoxic effects of PVP-AuNPs on HeLa cells were proven using cell viability and staining methods, thereby verifying their ability to cause cell death. Additional investigation is required to comprehend the

precise molecular processes that contribute to the suppression of cell growth, thereby facilitating the utilization of biosynthesized PVP-AuNPs as agents for preventing and treating cancer. PVP-AuNPs display promising antibacterial properties at higher concentrations, and their effectiveness across different bacterial strains suggests potential applications in antimicrobial formulations.

ACKNOWLEDGEMENT

I would like to sincerely thank the departments of chemistry at Gokul Global University and Hemchandracharya North Gujarat University for giving us the tools, direction, and encouragement I needed to complete my research. Their support and knowledge have been crucial to finishing our job.

Conflicts of interest

The authors declare that there are no conflicts of interest regarding the publication of this paper.

REFERENCES

1. Mai XT.; Tran MC.; Hoang AQ.; Nguyen PD.; Nguyen TH.; Tran HN.; Nguyen PT. Gold nanoparticles from *Celastrus hindsii* and HAuCl_4 : Green synthesis, characteristics, and their cytotoxic effects on HeLa cells., *Green Processing and Synthesis.*, **2021**, *10*(1), 73-84.
2. Dubey SP.; Lahtinen M.; Särkkä H.; Sillanpää M. Bioprospective of *Sorbus aucuparia* leaf extract in development of silver and gold nanocolloids. *Colloids and Surfaces B: Biointerfaces.*, **2010**, *80*(1), 26-33.
3. Castro L.; Blázquez ML.; Muñoz JA.; González F.; García-Balboa C.; Ballester A. Biosynthesis of gold nanowires using sugar beet pulp., *Process Biochemistry.*, **2011**, *46*(5), 1076-82.
4. Philip D. Green synthesis of gold and silver nanoparticles using *Hibiscus rosa sinensis*. *Physica E: Low-Dimensional Systems and Nanostructures.*, **2010**, *42*(5), 1417-24.
5. Bezerra TT.; de Almeida MO.; de Amorim Lima NM.; de Castro Rodrigues NL.; Ribeiro VG.; Teixeira MJ.; Carbone L.; Mele G, Lomonaco D.; Mazzetto SE. *In vitro* antileishmanial activity of sustainable anacardic acid and cardol based silver nanoparticles on *L. braziliensis*., *International Journal of Pharmaceutics.*, **2022**, *619*, 121698.
6. Kaur B.; Markan M.; Singh M. Green synthesis of gold nanoparticles from *Syzygium aromaticum* extract and its use in enhancing the response of a colorimetric urea biosensor., *BioNanoScience.*, **2012**, *2*, 251-8.
7. Sunderam V.; Thiyagarajan D.; Lawrence AV.; Mohammed SS.; Selvaraj A. *In-vitro* antimicrobial and anticancer properties of green synthesized gold nanoparticles using *Anacardium occidentale* leaves extract., *Saudi Journal of Biological Sciences.*, **2019**, *26*(3), 455-9.
8. Philip D.; Unni C.; Aromal SA.; Vidhu VK. *Murraya koenigii* leaf-assisted rapid green synthesis of silver and gold nanoparticles. *Spectrochimica Acta Part A: Molecular and Biomolecular Spectroscopy.* 2011, *78*(2), 899-904.
9. Behl A.; Chhillar AK. Nano-based drug delivery of anticancer chemotherapeutic drugs targeting breast cancer., *Recent patents on anti-cancer drug discovery.*, **2023**, *18*(3), 325-42.
10. Salam HA.; Sivaraj R.; Venckatesh RJ. Green synthesis and characterization of zinc oxide nanoparticles from *Ocimum basilicum* L. var. *purpurascens* Benth.-Lamiaceae leaf extract., *Materials letters.*, **2014**, *131*, 16-8.
11. Chandran SP.; Chaudhary M.; Pasricha R.; Ahmad A.; Sastry M. Synthesis of gold nanotriangles and silver nanoparticles using *Aloe vera* plant extract., *Biotechnology progress.*, **2006**, *22*(2), 577-83.
12. Talib A.; Khan MS.; Gedda G.; Wu HF. Stabilization of gold nanoparticles using natural plant gel: A greener step towards biological applications., *Journal of Molecular Liquids.*, **2016**, *220*, 463-7.
13. Philip D. Honey mediated green synthesis of gold nanoparticles., *Spectrochimica Acta Part A: Molecular and Biomolecular Spectroscopy.*, **2009**, *73*(4), 650-3.
14. Nakkala JR.; Mata R.; Bhagat E.; Sadras SR. Green synthesis of silver and gold nanoparticles from *Gymnema sylvestre* leaf extract: study of antioxidant and anticancer activities., *Journal of Nanoparticle Research.*, **2015**, *17*, 1-5.
15. Kamala Priya MR.; Iyer PR. Anticancer studies of the synthesized gold nanoparticles against MCF 7 breast cancer cell lines., *Applied nanoscience.*, **2015**, *5*(4), 443-8.
16. Ayyanar M.; Ignacimuthu S. Ethnobotanical survey of medicinal plants commonly used by Kani tribals in Tirunelveli hills of Western Ghats., India. *Journal of ethnopharmacology.*, **2011**, *134*(3), 851-64.
17. Pedersen ME.; Vestergaard HT.; Hansen SL.; Bah S.; Diallo D.; Jäger AK. Pharmacological screening of Malian medicinal plants used against epilepsy and convulsions., *Journal of Ethnopharmacology.*, **2009**, *121*(3), 472-5.
18. Karthi R.; Nagaraj S.; Arulmurugan P, Seshadri S.; Rengasamy R.; Kathiravan K. *Gymnema sylvestre* R. Br. suspension cell extract show antidiabetic potential in Alloxan induced diabetic albino male rats., *Asian Pacific Journal of Tropical Biomedicine.*, **2012**, *2*(2), S930-3.
19. Wu X.; Mao G.; Fan Q.; Zhao T.; Zhao J.; Li F.; Yang L. Isolation, purification, immunological and anti-tumor activities of polysaccharides from *Gymnema sylvestre*., *Food research international.*, **2012**, *48*(2), 935-9.

20. Jk G. Medicinal plants of India with antidiabetic potential., *J Ethnopharmacol.*, **2002**, *81*, 81-100.
21. Mai XT.; Tran MC.; Hoang AQ.; Nguyen PD, Nguyen TH.; Tran HN.; Nguyen PT. Gold nanoparticles from *Celastrus hindsii* and HAuCl_4 : Green synthesis, characteristics, and their cytotoxic effects on HeLa cells., *Green Processing and Synthesis.*, **2021**, *10*(1), 73-84.
22. Chen L.; Niu X.; Fan X.; Liu Y.; Yang J.; Xu X.; Zhou G.; Zhu B.; Ullah N.; Feng X. Highly absorbent antibacterial chitosan-based aerogels for shelf-life extension of fresh pork., *Food Control.*, **2022**, *136*, 108644.
23. Azzam AM.; Hazaa MM.; El Saeed AM.; Abdel-Naem MA. Antibacterial activity of Cu@ Ag nanocomposites against water bacterial pollution., *Journal of Basic and Environmental Sciences.*, **2017**, *4*(1), 85-9.
24. Haiss W.; Thanh NT.; Aveyard J.; Fernig DG. Determination of size and concentration of gold nanoparticles from UV-Vis spectra., *Analytical chemistry.*, **2007**, *79*(11), 4215-21.
25. Morsi MA.; Abdelghany AM. UV-irradiation assisted control of the structural, optical and thermal properties of PEO/PVP blended gold nanoparticles., *Materials Chemistry and Physics.*, **2017**, *201*, 100-12.
26. Ghosh S.; Patil S.; Ahire M.; Kitture R.; Gurav DD.; Jabgunde AM.; Kale S.; Pardesi K.; Shinde V.; Bellare J.; Dhavale DD. *Gnidia glauca* flower extract mediated synthesis of gold nanoparticles and evaluation of its chemocatalytic potential., *Journal of Nanobiotechnology.*, **2012**, *10*, 1-9.
27. Singh M.; Kalaivani R.; Manikandan S.; Sangeetha N.; Kumaraguru AK. Facile green synthesis of variable metallic gold nanoparticle using *Padina gymnospora*, a brown marine macroalga., *Applied Nanoscience.*, **2013**, 145-51.
28. Singh AK.; Srivastava O. One-step green synthesis of gold nanoparticles using black cardamom and effect of pH on its synthesis., *Nanoscale research letters.*, **2015**, *10*, 1-2.
29. Malik S.; Niazi M.; Khan M.; Rauff B.; Anwar S.; Amin F.; Hanif R. Cytotoxicity study of gold nanoparticle synthesis using *Aloe vera*, honey, and *Gymnema sylvestre* leaf extract., *ACS omega.*, **2023**, *8*(7), 6325-36.
30. Chen M.; He Y.; Liu X.; Zhu J.; Liu R. Synthesis and optical properties of size-controlled gold nanoparticles., *Powder technology.*, **2017**, *311*, 25-33.
31. Raza MA.; Kanwal Z.; Rauf A.; Sabri AN.; Riaz S.; Naseem S. Size-and shape-dependent antibacterial studies of silver nanoparticles synthesized by wet chemical routes., *Nanomaterials.*, **2016**, *6*(4), 74.
32. Sunderam V.; Thiyagarajan D.; Lawrence AV.; Mohammed SS.; Selvaraj A. *In-vitro* antimicrobial and anticancer properties of green synthesized gold nanoparticles using *Anacardium occidentale* leaves extract., *Saudi Journal of Biological Sciences.*, **2019**, *26*(3), 455-9.
33. Ahmad B.; Hafeez N.; Bashir S.; Rauf A. Phytofabricated gold nanoparticles and their biomedical applications., *Biomedicine & Pharmacotherapy.*, **2017**, *89*, 414-25.
34. Tran N.; Le A.; Ho M.; Dang N.; Thi Thanh HH.; Truong L.; Huynh DP.; Hiep NT. Polyurethane/polycaprolactone membrane grafted with conjugated linoleic acid for artificial vascular graft application., *Science and Technology of Advanced Materials.*, **2020**, *21*(1), 56-66.
35. Ly TN.; Shimoyamada M.; Yamauchi R. Isolation and characterization of rosmarinic acid oligomers in *Celastrus hindsii* Benth leaves and their antioxidative activity., *Journal of agricultural and food chemistry.*, **2006**, *54*(11), 3786-93.
36. Pham DC.; Nguyen HC.; Nguyen TH.; Ho HL, Trinh TK.; Riyaphan J.; Weng CF. Optimization of Ultrasound Assisted Extraction of Flavonoids from *Celastrus hindsii* Leaves Using Response Surface Methodology and Evaluation of Their Antioxidant and Antitumor Activities., *BioMed research international.*, **2020**(1), *3*, 497-107.
37. Bui TT.; Vu MH.; Bui TT. Cytotoxicity and antioxidant effects of *Celastrus hindsii* benth. Leaf extract. *VNU Journal of Science: Medical and Pharmaceutical Sciences.*, **2020**, *36*(1).